DUCTILE FAILURE OF CRACKED MEMBER UNDER COMBINED LOADING OF MEMBRANE AND BENDING STRESSES

H. OKAMURA, M. KUROTOBI

Department of Mechanical Engineering, Faculty of Engineering, University of Tokyo, Bunkyo-ku, Tokyo, 113, Japan

SUMMARY

In the present status of structural design of reactor components, the design of the strength of structural member is essentially based on the collapse load in un-cracked state of the member, and partly referred to the strength for brittle fracture in its cracked state. However, it might be important to know the strength for ductile failure of cracked member in the design of most structural components except thick walled pressure vessels. The criterion for brittle fracture has been well established, and the fracture strength of cracked member with heavy section can be estimated by linear fracture mechanics through the fracture toughness K_{IC}. On the other hand, the criterion of ductile fracture of cracked member with thin section will be given by collapse load. Once the both criterions are revealed, the strength of cracked member with medium section might be hopefully estimated by a two-criteria-approach using the K_{IC} and the collapse load. From this standpoint of view, the collapse load of the edge-cracked member under the bending stress and the membrane stress has been investigated in the present paper. The materials used are two kinds of pressure vessel steels, equivalent to ASTM A533B cl. 1 and ASTM A516. The edge-cracked bars with crack-like notches were loaded eccentrically, and the collapse loads and the maximum carrying loads were measured.

The comparison of the collapse loads in experiments with the analytical solutions shows that the collapse loads under the combined bending and tensile loading can be satisfactorily estimated by the analytical solutions in the theory of plasticity. In addition, the curves of collapse load of cracked member are shown as a function of the ratio of the crack depth a to the thickness W on the P_m vs. (P_m+P_b) diagram, where P_m and P_b are primary membrane stress and bending stress respectively. One of the conclusions obtained from this diagram is that the member does not collapse as long as the crack depth is shallower than a quarter of the thickness, if the member is designed according to the design limit for the normal operating condition in ASME Code Sec. III ($P_m \leqq 1.5S_y$, $P_m+P_b \leqq S_y$, where S_y is the yield stress).

1. Introduction

As a minimum of the load carrying capacity and as an extreme of the brittle-ductile transition of fracture, the plastic collapse load is important to evaluate the strength of the cracked structural member. One of the present authors and others [1] have investigated experimentally and analytically the collapse limit and the load carrying capacity of the cracked column under the combined loading of the compressive membrance stress and the bending stress. Along the same line of the research, the present paper will reveal the collapse limit of the edge-cracked member under the combined effect of the tensile membrance stress P_m and the bending stress P_b.

2. Theoretical Results on the Collapse Load

Prior to the description of the experiment, the existing solutions of the collapse load will be shown here.

2.1 Collapse Limit of Un-cracked Member

The membrane stress P_m and the bending stress P_b are defined by the relations

$$P_m=F/W, \quad P_b=M/(W^2/6) \tag{1}$$

respectively, where W is the thickness of the member, F and M are the axial force and the bending moment per unit width referred to the center line of the thickness. In case of the non-hardening material with yield stress S_y, the limit of collapse is well known and expressed by the equation

$$P_b/1.5S_y+(P_m/S_y)^2=1, \qquad (-1\leqq P_m\leqq 1). \tag{2}$$

2.2 Collapse Limit of Cracked Member

Assume that the edge crack with depth a exists all through the width. As the axial force and the bending moment referred to the center line of the ligament with depth $W'=W-a$ are given by $F'=F$ and $M'=M-Fa/2$ respectively, the membrane stress P'_m and the bending stress P'_b referred to the ligament depth are defined and given by

$$P'_m\equiv F'/W'=(W/W')P_m, \qquad P'_b\equiv M'/(W'^2/6)=(W/W')^2P_b-3(W/W')(a/W')P_m \tag{3}$$

In case of pure bending of the member with crack-like notch, the slip line field of perfect solution is given by Green [2] and shown by solid lines in Fig. 1. The field consists of the uniform stress field (SQTQ'S')and the circular arcs (OQ and OQ'), and this yields an upper bound of collapse load, that is,

$$\text{Pure bending;} \qquad P_b/1.5S_y=L_o\fallingdotseq 1.2606, \qquad (P_m=0) \tag{4}$$

where L_o is well known as the plastic constraint factor for bending when the flank angle of the notch is zero.

When the compressive membrane stress $P_m(<0)$ is superimposed on P_b, the relative size of the uniform stress field increases compared with the size of the rigid hinge (OQ,OQ'), which is shown by I in Fig. 1. When the tensile stress $P_m(>0)$ is applied, the relative size of the uniform stress field decreases as is shown by II, and when P'_m/S_y approaches 0.552, the lower edge of the bar S_{II} approaches to the end of arc Q and the uniform stress fields vanishes. The perfect solution in these regions I and II can be easily obtained by considering the contribution of variation of the uniform stress field, and given as follows;

$$\text{Regions I \& II;}\quad P_b'/1.5S_y = L_o(1+P_m'/S_y)^2 - 2(1+P_m'/S_y)(P_m'/S_y)$$
$$\fallingdotseq 1.261 + 0.739P_m'/S_y - 0.521(P_m'/S_y)^2, \quad (-1 \leqq P_m'/S_y \leqq 0.552) \qquad (5)$$

This solution holds for a deep notch, and the limit of the application is given by the relation [3]

$$a/W \geqq 0.0543(1+P_m/S_y). \qquad (6)$$

In the range III where $0.552 < P_m'/S_y \leqq 1$, an optimum solution among upper bounds can be obtained by posulating the slip lines of arcs OQ and OQ′ and by changing the intersecting angle φ. The optimum angle changes from the original value 144.1° to 90° as P_m'/S_y changes from 0.552 to 1. A numerical solution of the optimum upper bound has been given in polinominal form by Shiratori et al. [4]. Fig. 5 shows the solution in the range III as well as those in the ranges I and II. The lower bound of the cracked member is given by the relation as eq. (2)

$$\text{Lower bound;}\quad P_b'/1.5S_y + (P_m'/S_y)^2 = 1, \quad (-1 \leqq P_m'/S_y \leqq 1) \qquad (7)$$

which is shown by the curve IV in Fig. 5.

3. Materials and Specimen Configulation

3.1 Materials

The materials tested are the pressure vessel steels, JIS SQV2A (corresponding to ASTM A533 B cl.1) and JIS SGV49N (ASTM A516), whose mechanical properties and chemical compositions on MIL sheets are shown in Table I and Table II respectively. The yield were cut from the plates in the perpendicular direction to the rolling direction. The specimens stresses to this direction are different from the values on MIL sheets, but are 33.1 and 49.7 kg/mm^2 respectively, which are used as S_y in the analysis of experimental data.

3.2 Specimen Configulation

In order to apply both of P_m' and P_b' simultaneously, the single-edge-notched specimens were eccentrically loaded by pins. The configulation of the specimens and the eccentricity are shown are shown in Fig. 2. The crack-like notch is induced mechanically, whose width and root radius are approximately 0.2 and 0.1 mm respectively. The combination of the eccentricity e and the crack depth ratio a/W are shown in Table III.

4. Experimental Results

During the tensile tests of the specimen, the displacement at the loading point u, that is, the elongation between two pins, and the angular deformation between the ends of the specimen θ were measured, and the bending moment were calculated from the tensile load and the eccentricity correcting by the measured lateral deflection.

Fig. 3 shows some examples of the diagrams of P_m vs. u and P_b vs. θ. There could be many definitions of the collapse, but for conveniance' sake, the collapse load is tentatively determined by the load at the displacement of twice of that at the proportional limit on P_m vs. u diagram. Even if we adopted the criterion of twice compliance, there could not be much difference in the collapse load. The points at the collapse and at the maximum membrane stress are denoted by the circle and the triangle respectively on the diagram.

Fig. 4 shows all of the trajectories of P_m' and P_b' together with the collapse points and the maximum P_m' points. The upper bound and the lower bound shown in Fig. 5 are also drawn in this figure. After the specimen collapses near the upper bound curve, the ratio of P_b'/P_m' decreases because of the lateral deflection, and then the P_m reaches its maximum value.

5. Discussions

It is concluded from the results shown in Fig. 4 that the upper bound solutions presented above can be used as a satisfactory criterion on the on-set of the collapse, and that the cracked member can sustain load far beyond the upper bound solutions. In Fig. 6, the upper bound solutions are shown as a function of the crack depth ratio a/W on P_m vs. P_b+P_m diagram instead of P_m' vs. P_b' diagram. The outer closed curve of parabolas is the collapse limit of un-cracked member given by eq. (2). The inner hexagon shows the design limit in ASME Code Sec. III for the normal operating condition, namely,

$$|P_m|=(2/3)S_y, \qquad |P_m|+|P_b|=S_y \tag{8}$$

Even if a crack through the width exists in a member designed within the above design limit, the member can sustain the design load without appreciable plastic deformation as long as $a/W<1/4$. For the part-through surface crack with maximum depth of a , the above criterion for collapse is too conservative not only because of the limitation of the crack length but also of the constraint by the uncracked section. There are some differences of the behaviour of trajectories in both materials up to maximum P_m', as is shown in Fig. 4. In case of SGV49N, the maximum membrane stresses across the ligament are nearly equal to the ultimate tensile strength S_u. On the other hand, in case of SQV2A, the yield ratio of the material S_y/S_u is smaller than that of the other material and, in addition, the maximum P_m' is sometimes greatly less than S_u. The reason of the difference is not yet clarified, but possibly because of a stable growth of crack in SQV2A.

The ductile failure of the cracked member with thin section and the brittle failure of that with heavy section can be evaluated by the collapse and the fracture toughness K_{IC} respectively. The evaluation of the failure of cracked member with medium section is the problem in Non-linear Fracture Mechanics, which is not yet solved. To the purpose of a rough estimation of the strength in the range of medium section, it is worth while to check the validity of the application of the universal failure curve proposed by Dowling and Townley[5]. Let the collapse stress and the fracture stress estimated through K_{IC} under a given P_b/P_m ratio be P_m^c and P_m^f respectively, and the membrane stress at fracture P_m is given by the universal failure curve based on the plastic zone correction by the Dugdale model;

$$P_m \approx P_m^c \frac{2}{\pi} \cos^{-1}\left[\exp\left\{-\frac{\pi^2}{8}(P_m^f/P_m^c)^2\right\}\right], \tag{9}$$

This relation can be approximated by the following relation based on a simpler plastic zone correction;

$$P_m \approx \mathrm{Min.}\left[P_m^c,\ P_m^c/\sqrt{0.5+(P_m^c/P_m^f)^2}\right] \tag{9'}$$

The validity of the eq. (9) should be checked in future research.

ACKNOWLEDGEMENTS- The authours wish to express their gratitude to Mr. Tachio Takano of University of Tokyo for his assistances in managing the research. This work has been done as a part of EDR Research Project.

References

[1] Okamura, H., Watanabe, K., Takano, T., "Deformation and Strength of Cracked Member Under Bending Moment and Axial Force," Engineering Fracture Mechanics, vol.7 (1975) 531.

[2] Green, A.P., "The Plastic Yielding of Notched Bars Due to Bending," Quart. J. Mech. Appl. Maths., 6 (1953) 223.

[3] Kurotobi, M., "Collapse Strength of Cracked Members of Ductile Material" Master Thesis, Univ. of Tokyo (March, 1979)

[4] Shiratori, M., Miyoshi, T., "Plastic Constraint of SEN Specimen and its J-integral ," JSME paper, No. 780-9 (July, 1978) 63.

[5] Harrison, R.P., Fracture Mechanics in Engineering Practice, (1977) 69, Applied Science Publishers.

Table I Mechanical Properties

Material	Position	Yield Strength 0.2% offset (kg/mm^2)	Tensile Strength (kg/mm^2)	Elongation (%)	Red. of Area (%)
SGV49N	—	39	53	29	—
SQV2A	Top.	46.2	62.3	27.6	63.6
	Bot.	48.4	63.6	26.5	67.7

Table II Chemical Composition (Wt. %)

Material	Position	C	Si	Mn	P	S	Ni	Cr	Cu	Mo	V
SGV49N	—	.16	.27	1.11	.016	.005	.20	.01	.01	.19	.05
SQV2A	Top.	.17	.26	1.39	.007	.007	.68	.20	.04	.49	trace
	Bot.	.17	.27	1.38	.008	.006	.67	.20	.04	.49	trace

Table III Test Conditions

(a) Material ; SQV2A

Test No.	Specimen	e(mm)	a/W
1	Q - 1 - 1	-0.02	0.147
2	Q - 1 - 2	0.14	0.201
3	Q - 1 - 3	0.10	0.246
4	Q - 1 - 4	0.21	0.301
5	Q - 2 - 1	0.79	0.158
6	Q - 2 - 2	0.85	0.316
7	Q - 2 - 3	0.82	0.194
8	Q - 2 - 4	0.84	0.320
9	Q - 3 - 2	1.84	0.210
10	Q - 3 - 3	1.93	0.252
11	Q - 3 - 4	1.95	0.286
12	Q - 3 - 5	1.86	0.152
13	Q - 4 - 1	3.88	0.164
14	Q - 4 - 2	3.93	0.203
15	Q - 4 - 3	3.83	0.252
16	Q - 4 - 4	3.88	0.300
17	Q - 5 - 1	7.83	0.151
18	Q - 5 - 2	7.76	0.203
19	Q - 5 - 3	7.93	0.243
20	Q - 5 - 4	7.90	0.304
21	Q - 3 - 6	-1.80	0.303

(b) Material ;SGV49N

Test No.	Specimen	e(mm)	a/W
1	G - 1 - 1	- 0.42	0.153
2	G - 1 - 2	0.02	0.249
3	G - 1 - 3	0.02	0.215
4	G - 1 - 4	0.01	0.279
5	G - 2 - 2	0.92	0.238
6	G - 2 - 3	0.90	0.198
7	G - 2 - 6	0.96	0.304
8	G - 2 - 7	0.87	0.193
9	G - 2 - 8	0.90	0.154
10	G - 3 - 1	1.86	0.148
11	G - 3 - 2	1.90	0.219
12	G - 3 - 3	1.87	0.319
13	G - 3 - 4	1.90	0.262
14	G - 3 - 5	1.89	0.231
15	G - 3 - 6	1.90	0.196
16	G - 3 - 7	1.91	0.149
17	G - 3 - 8	1.86	0.290
18	G - 4 - 1	3.95	0.182
19	G - 4 - 2	3.93	0.226
20	G - 4 - 3	3.89	0.250
21	G - 4 - 4	3.87	0.295
22	G - 5 - 2	8.04	0.358
23	G - 5 - 3	7.96	0.240

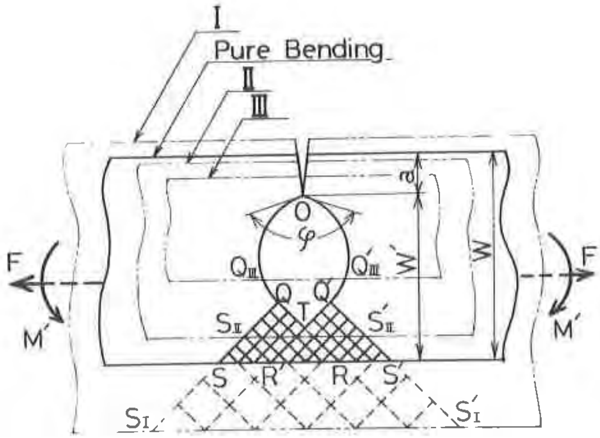

Fig. 1 Slip line field in edge-cracked member

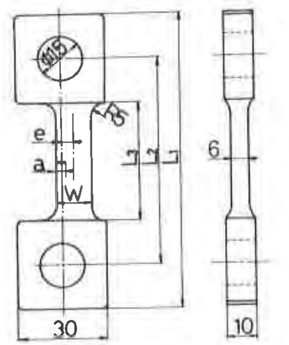

material	L_1	L_2	L_3	W
SGV49N	100	70	40	12
SQV2A	96	66	36	12

type	1	2	3	4	5
e	0	1	2	4	8

unit ; mm

Fig. 2 Specimen configulation

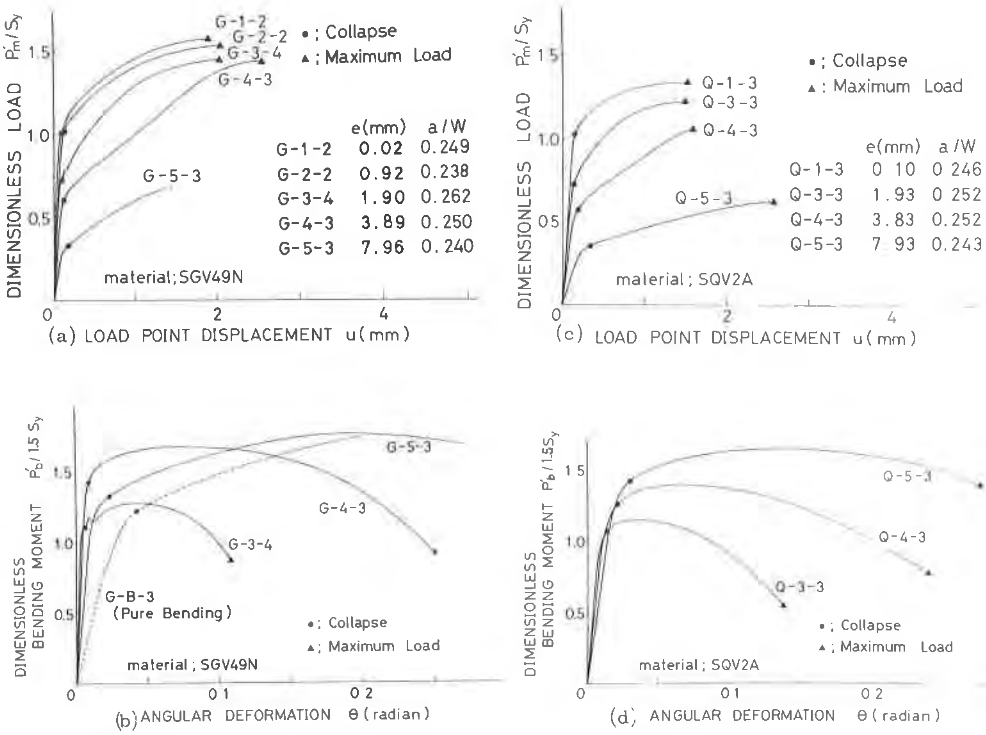

Fig. 3 Examples of load-displacement diagrams

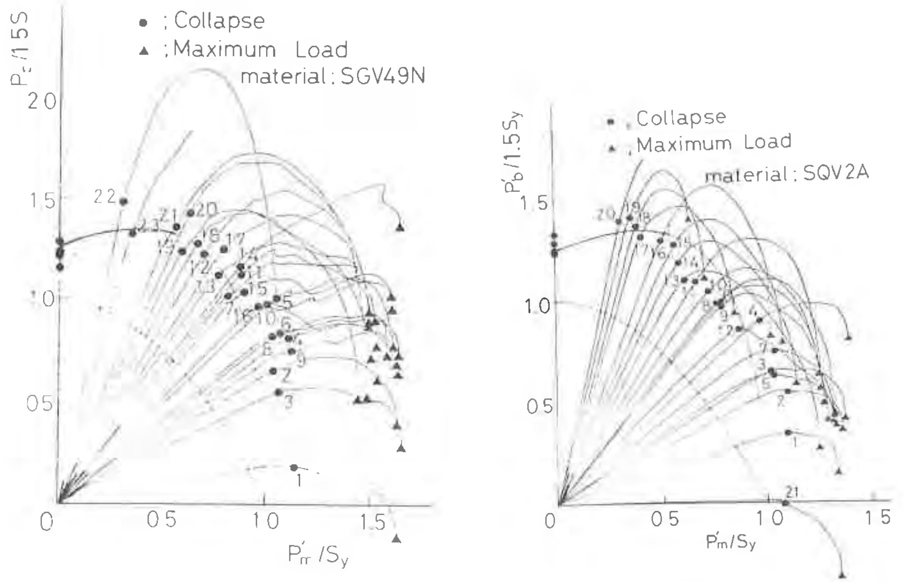

Fig. 4 Experimental results on the collapse limits and the maximum membrane stress

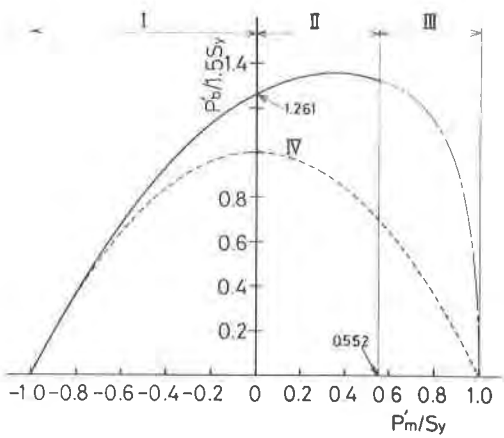

Fig. 5 Upper and lower bounds of collapse loads

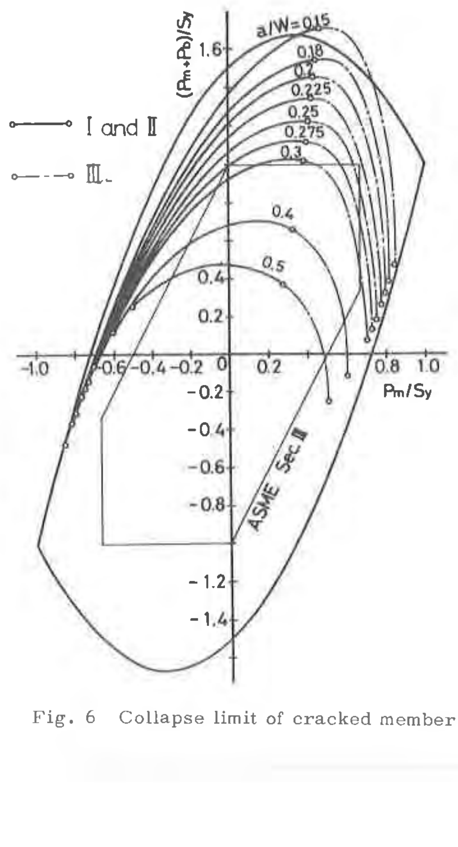

Fig. 6 Collapse limit of cracked member